

REPORT DOCUMENTATION PAGE

Form Approved
OMB No. 0704-0188

Public reporting burden for this collection of information is estimated to average 1 hour per response, including the time for reviewing instructions, searching existing data sources, gathering and maintaining the data needed, and completing and reviewing this collection of information. Send comments regarding this burden estimate or any other aspect of this collection of information, including suggestions for reducing this burden to Department of Defense, Washington Headquarters Services, Directorate for Information Operations and Reports (0704-0188), 1215 Jefferson Davis Highway, Suite 1204, Arlington, VA 22202-4302. Respondents should be aware that notwithstanding any other provision of law, no person shall be subject to any penalty for failing to comply with a collection of information if it does not display a currently valid OMB control number. PLEASE DO NOT RETURN YOUR FORM TO THE ABOVE ADDRESS.

1. REPORT DATE (DD-MM-YYYY) 12-20-2006	2. REPORT TYPE FINAL REPORT	3. DATES COVERED (From - To) 01-12-02 - 30-09-06
---	--------------------------------	---

4. TITLE AND SUBTITLE Adaptive Optics for Turbulent Shear Layers	5a. CONTRACT NUMBER
	5b. GRANT NUMBER F49620-03-1-0019
	5c. PROGRAM ELEMENT NUMBER

6. AUTHOR(S) ERIC J. JUMPER	5d. PROJECT NUMBER
	5e. TASK NUMBER
	5f. WORK UNIT NUMBER

7. PERFORMING ORGANIZATION NAME(S) AND ADDRESS(ES) DEPARTMENT OF AEROSPACE AND MECHANICAL ENGINEERING UNIVERSITY OF NOTRE DAME NOTRE DAME, IN 46556	8. PERFORMING ORGANIZATION REPORT NUMBER
---	---

9. SPONSORING / MONITORING AGENCY NAME(S) AND ADDRESS(ES) AIR FORCE OFFICE OF SIENTIFIC RESEARCH, AFOSR/NA <i>Rhett Jeffries</i> 875 North Randolph St. Suite 325, Room 3112 ARLINGTON, VA 22203-1768	10. SPONSOR/MONITOR'S ACRONYM(S)
	11. SPONSOR/MONITOR'S REPORT NUMBER(S)

12. DISTRIBUTION / AVAILABILITY STATEMENT <i>Approved for public release. Distribution unlimited</i>	AFRL-SR-AR-TR-07-0218
---	-----------------------

13. SUPPLEMENTARY NOTES

14. ABSTRACT This report describes aero-optic research at the University of Notre Dame. When a laser beam propagates through a variable-index-of-refraction, turbulent fluid, its wavefront becomes aberrated, reducing associated optical-system performance. For flight Mach numbers as low as 0.3 Mach, turbulence in the flow past the aircraft become important in aberrating wavefronts (aero-optics). This report reviews the mechanisms responsible for these aberrations in free-shear-layer flows, the so-called Weakly-Compressible Model, which identifies the coherent structures in the flow as the major contributor to the flow's aberrating character. The report describes the use of flow control to regularize these coherent structures so as to reduce the bandwidth required by an adaptive-optic system to mitigate their effects. The report describes two historic demonstrations of the combined use of flow control and feed-forward adaptive optics to correct the aberrations imposed on an otherwise collimated laser beam projected through a heated jet and a Mach 0.8 free shear layer, respectively.

15. SUBJECT TERMS
Aero-Optics, Fluid-Optic Interactions, Adaptive Optics, Wavefront Sensing, Compressible Shear Layers, Flow Control, Mixing Layers, Turbulence, the Weakly-Compressible Model

16. SECURITY CLASSIFICATION OF: UNCLASSIFIED			17. LIMITATION OF ABSTRACT UL	18. NUMBER OF PAGES 24 including title page	19a. NAME OF RESPONSIBLE PERSON Dr. Rhett Jefferies, LtCol
a. REPORT UNCLASSIFIED	b. ABSTRACT UNCLASSIFIED	c. THIS PAGE UNCLASSIFIED			19b. TELEPHONE NUMBER (include area code) (703) 696-6961

Adaptive Optics for Turbulent Shear Layers

Final Report

AFOSR Grant F49620-03-1-0019

**Period Covered:
1 December 2002 – 30 September 2006**

Principal Investigator: Eric J. Jumper

Center for Flow Physics and Control
Hessert Laboratory
Department of Aerospace and Mechanical Engineering
University of Notre Dame
Notre Dame, Indiana 46556
USA

(574) 631-7680
FAX: (574) 631-8355

Email: jumper.1@nd.edu

20 December 2006

ABSTRACT

When a laser beam with an otherwise planar optical wavefront, is made to propagate through a turbulent, variable-index flow field, the beam's wavefront is imprinted with a time-varying aberration over its aperture (beam diameter). These dynamic aberrations degrade the ability for the beam to be focused in the far field. In the case of a laser propagated from an airborne platform, the far field could be anywhere from kilometers to hundreds of kilometers away. The effectiveness of an airborne laser system depends on the beam-control system being able to hold a spot on the far-field aim point, which exceeds a minimum intensity. The beam's intensity in the far field is directly dependent on how well it can be focused. In general, there are two distinct regimes of variant-index flows that contribute to the focusability: the first is the beam's path from just outside the flowfield surrounding the aircraft, through the intervening atmosphere, to the far field; and the second is the flow traversed by the beam within the immediate vicinity of the aircraft. The first regime is referred to as "atmospheric propagation." This grant effort specifically addressed the second regime, the optical-propagation problem in the immediate vicinity of an airborne platform; this regime of the optical-propagation problem is referred to as "aero-optics." In particular, this effort was concerned with building the knowledge base needed to actively mitigate wavefront aberrations due to laser propagation through *separated shear layers*. AFOSR-funded research at Notre Dame has shown that, although propagation through attached turbulent boundary layers can reduce the average on-axis intensity in the far field by 5 – 30%, this reduction in intensity pales in comparison to propagation through a separated shear layer, which can reduce the intensity in the far field by more than 95%. The problem of understanding how to deal with propagation through a separated shear layer has gained new significance in recent years with the DoD's interest in the design issues related to placing shorter-wavelength lasers on aircraft.

The Notre Dame AFOSR efforts in aero-optics, including the work reported on here, are a success story in research investment, which began approximately a decade ago. At that time, aero-optics was considered to be a mature topic, assumed to be treatable only as a stochastic process, and addressable only through statistical methods. This meant that, at best, aero-optics could provide only *the ability to estimate the reduction in lethality that might be incurred due to firing through the flow field next to the aircraft*. Through Notre Dame's AFOSR-sponsored efforts in aero-optics, knowledge has been moved to a cause-and-effect understanding of aero-optics and this knowledge has led to a number approaches to mitigating its deleterious effects. The report details the use of the knowledge and techniques developed in previous grants to the specific task of regularizing the coherent structures in turbulent shear flows and making use of the repeating wavefront aberration patterns due to laser propagation through the regularized shear layers to demonstrate the first-ever adaptive-optic correction of the beam. Three milestone demonstrations are reported on. The first is the adaptive-optic correction of a laser propagated through a heated jet. The second is the demonstration of the first regularization of a flight-relevant, high-Mach-number, subsonic shear layer. And the third is the first-ever adaptive-optic correction of a 8 inch laser propagated through a Mach 0.8 free shear layer.

TABLE OF CONTENTS

	Page
ABSTRACT	i
TABLE OF CONTENTS	ii
I. INTRODUCTION	3
Objectives	3
Approach	4
II. BACKGROUND	5
Aero-Optics	5
Characteristics of Aero-Optic Aberrations	6
Cause of Aero-Optic Aberrations	7
Flow-Control, Feed-Forward Adaptive-Optic Foundations	9
III. RESULTS	11
Heated-Jet Demonstration	11
Regularized Shear Layer	11
Adaptive-Optic Demonstration	11
Shear Layer Forcing	15
Adaptive-Optic Correction	18
IV. CONCLUSIONS	20
V. REFERENCES	21

I. INTRODUCTION

When a collimated laser beam of wavelength $\sim 1 \mu\text{m}$ propagates through a separated shear layer with a convective Mach number as low as 0.15 (high speed side at $M = 0.3$) the beam's wavefront is aberrated to the point that its focused intensity can be reduced by more than 50% of its diffraction-limited intensity. The study of the aberrating effect of shear flows is referred to as *Aero-Optics*.¹ Notre Dame has been studying aero-optics since 1993 (F49620-93-0163, F49620-97-1-0489 and F49620-00-1-0025) and has made many breakthroughs. The Notre Dame efforts have moved the understanding of aero-optics from a statistically-based, time-averaged, optical-path-difference (OPD) approach, based on statistical, fluid-mechanical measurements, to a formal, cause-and-effect understanding of optical propagation through boundary and shear layers.^{1,2,3} The work reported here made use of the results of these previous grants, in particular the knowledge of the aberrating physics, various high-bandwidth wavefront-sensing instruments developed at Notre Dame, techniques developed using other commercially-available instruments, and our high-bandwidth deformable mirror, acquired under a DURIP grant as part of our high-bandwidth adaptive optics system to demonstrate two important milestones in adaptive optics. The second and most important milestone, correcting a laser beam projected through a Mach 0.8 shear layer, was made possible by a ten month cost extension of this grant to 30 September 2006 supported by AFRL/DE and AFRL/VA.

Objectives. As will be described in detail in the Background section, aero-optic aberrations in weakly-compressible flows are caused by coherent structures that form in turbulent flows. These coherent structures are characterized by highly curved and closed streamlines in the convecting frame accompanied by low pressure, density and temperature wells that have concomitant regions of low index-of-refraction regions and high-index regions in the connecting braids of the flow with coherence lengths that are characterized by the dimensions of the coherent structures. In free shear layers, these most-optically-degrading coherent structures form naturally under the influence of the Kelvin-Helmholtz instability. In their natural state, these structures, which align along the spanwise direction, form in free shear layers irregularly, starting with small, high spatial- and temporal-frequency structures closest to the separation point and increase in size, to lower spatial- and temporal-frequency structures as the layer convects downstream from its separation point.⁴ Using traditional approaches to adaptive optics, the bandwidth requirements for sensing the aberrations due to optical propagation through the shear layer, translation into appropriate conjugate wavefronts, and application of the required voltages to a deformable mirror of sufficient response bandwidth is well beyond the capabilities of adaptive-optic systems presently contemplated. It has long been known that shear layers are receptive forcing at their origin to either rapidly increase their thickness or cause their thickness to "stabilize." This research inferred that these regions of thickness stabilization were due to the creation of regular coherent-structure patterns that were periodic and thus predictable; in fact, this work confirmed that this inference was correct. Based on the presumption that "*regularization*" was possible, the *first objective* of this effort was to develop a combined flow-control, feed-forward

adaptive-optic scheme capable of correcting for laser propagation through an aberrating shear layer and demonstrate this approach on laser propagation through a heated jet. The *second objective* was to demonstrate *regularization* of a Mach 0.8 shear layer. This second objective was no small task since stabilization (from which we inferred meant regularization) of such a high-Mach-number shear layer had never been demonstrated. Made possible by a cost extension to this grant, an *additional objective* to demonstrate the combined flow-control, feed-forward adaptive-optic correction for a laser propagated through a Mach 0.8 shear layer was added.

Approach. The approach to accomplish the *first objective* was to make use of a two-dimensional heated jet that was shown in an earlier grant to be robustly regularizable over a short distance near the nozzle exit plane using acoustic forcing. An 18 mm, 0.63 μm collimated laser beam was propagated through the near-exit-plane regularized heated jet and its aberrated wavefronts were recorded using a wavefront sensor, phase-locked to the forcing frequency. In this way a phase-averaged wavefront-pattern record over a full repetition cycle of the regularized aberration was made. These wavefront patterns were converted to a smooth voltage pattern that was a function of time, and this time-dependent voltage pattern was applied to Notre Dame's deformable mirror. The aberrated beam was then reflected off the deformable mirror and its residual wavefront error was recorded and examined as a function of amplitude and phase delay of the applied voltage waveform signal.

The *second objective*, to demonstrate regularization of a high-Mach shear layer, was accomplished by exploring a series of flow-control actuators and evaluating their effectiveness in regularizing the shear layer. Eventually, a voice-coil actuator was shown to robustly control the shear layer. The success in forcing regularization of the shear layer was assisted by performing numerical simulations of the flow. The effectiveness in regularizing the shear layer was evaluated using wavefront sensors and hot wires. This second objective required the design and construction of an entirely new shear layer facility.

The *additional objective* was accomplished by adapting the approach used for the heated jet to the regularized compressible shear layer. This required the development of a new optical set up.

II. BACKGROUND

Aero-Optics. The projection of a collimated laser beam (or incoming optical wavefront), of “viewing aperture” A_p , through a turbulent flowfield with index-of-refraction variations, leads to a time-varying aberration of its otherwise-planar, optical wavefront. These aberrations lead to a reduction in performance of an optical system making use of the optical “information” contained over the viewing aperture. Systems concerned with such reduction in performance include, but are not limited to, airborne imaging systems and airborne laser irradiating systems. These latter systems include airborne laser weapons such as the AirBorne Laser (ABL) theater ballistic defense system, the advanced concept technology demonstrator Airborne Tactical Laser (ATL), and Tactical Aircraft High Energy Laser systems (TAHEL), as well as airborne free-space communication systems.

A system’s performance reduction (induced by turbulent, variant-index flowfields) can be quantified by analysis of the far-field irradiance pattern.⁵ The irradiance pattern is the instantaneous intensity pattern at the target, $I(x,y,t)$, where $(0,0)$ would indicate the center of the aim point. The extent to which the on-axis intensity is reduced as a function of time, $I(0,0,t)$, when divided by the highest possible on-axis intensity without aberrations (referred to as the diffraction-limited intensity), I_o , is expressed as the Strehl ratio, S_t ,

$$S_t(t) = \frac{I(0,0,t)}{I_o} \quad (1)$$

The reduction in Strehl ratio due to time-varying, aberrating flowfields can occur over short path lengths in the *near field* (i.e., path length, z , on the order of A_p), or it can occur over extended paths (i.e., path lengths, z , much larger than A_p). The former, short-path (near-field) aberration is usually termed *aero-optics* and the latter, long-path aberrations are usually termed *atmospheric propagation*. These classifications have their origin in the specific applications with which they are associated [see Refs. 6 and 7, for example]. It has long been known that placing a conjugate waveform on the beam prior to its transmission through the aberrating medium results in the emergence of a planar-wavefront beam as it leaves the medium; systems that sense the aberration, construct and apply the proper conjugate waveform at regular time intervals are termed *adaptive-optic systems*, and the study of such systems is known as *adaptive optics*.⁸ The determination of the design requirements for such systems depends on understanding the spatial and temporal frequencies of the distorted optical wavefront for the applicable aberrating flowfields.

Over the last two decades progress has been made in both measuring the wavefront dynamics for the atmospheric propagation problem and using this information for designing and applying adaptive-optic equipment and techniques.⁹ For aero-optic problems, on the other hand, until Notre Dame’s successful demonstrations reported here, *no adaptive optic correction for the aero-optic problem was ever demonstrated*. The reason for the inability to correct for aero-optic aberrations prior to work reported here is that the required spatial and temporal frequencies associated with aero-optic problems are at least an order of magnitude greater than those correctable by the traditional approach to designing adaptive-optic systems, even for relatively-slow laboratory flows.¹⁰ As such, the main research thrust in aero-optics until the early to mid 1990’s had been to attempt to quantify the time-averaged phase variance (or root-mean-square Optical Path Difference, OPD_{rms} , which is related to the phase variance through the wave number). Once obtained

by whatever means, the phase variance was used to compute *an estimate* of the system degradation imposed by the near-field aberrations using the large-aperture approximation.¹ These statistical methods gave no information useful to the design of adaptive-optic systems required to correct aero-optic aberrations. Research at Notre Dame supported by AFOSR has focused exclusively on the *aero-optics problem*, with an emphasis on understanding how *adaptive optics* can be applied to the problem. As will be described later in this report, Notre Dame has introduced flow control into the adaptive-optic paradigm and developed a feed-forward approach that has now demonstrated a historic first, the adaptive-optic correction of a laser propagated through an otherwise devastating Mach 0.8 free shear layer.

Characteristics of Aero-Optic Aberrations. During a previous AFOSR grant, Notre Dame used an in-house developed wavefront sensor to measure the first-ever, time-resolved wavefront dynamics for laser propagation through the Mach 0.8 compressible shear layer at the Arnold Engineering Development Center (AEDC).^{11,12} Figure 1 shows two example time series of measured one-dimensional wavefronts from those tests (5 cm aperture); these data were taken at two stations, Station 1, right at the splitter plate, and Station 2, half a meter downstream from the splitter plate. What is most noteworthy in the data shown in Fig. 1 is the difference in aberration extent between the Station 1 and Station 2 data. The Station 1 data is due to the turbulent boundary layer feeding the shear layer and/or over the extraction window. Even without boundary layer treatment to remove these aberrations, the level of aberration is quite low. For a one-micron-wavelength beam the Strehl ratio can be estimated to be ~ 0.91 using the large-aperture approximation. It might be noted that the Station 2 data contains cyclic tilt, but even when this is removed, computed far-field patterns yielded a time-averaged Strehl ratio of < 0.1 .¹² Realistic beam diameters for a HEL system will not be smaller than 20 cm, and when the wavefronts are extended to apertures, A_p , greater than 20 cm the OPD_{rms} increases to 0.43 mm, further reducing the Strehl ratio.

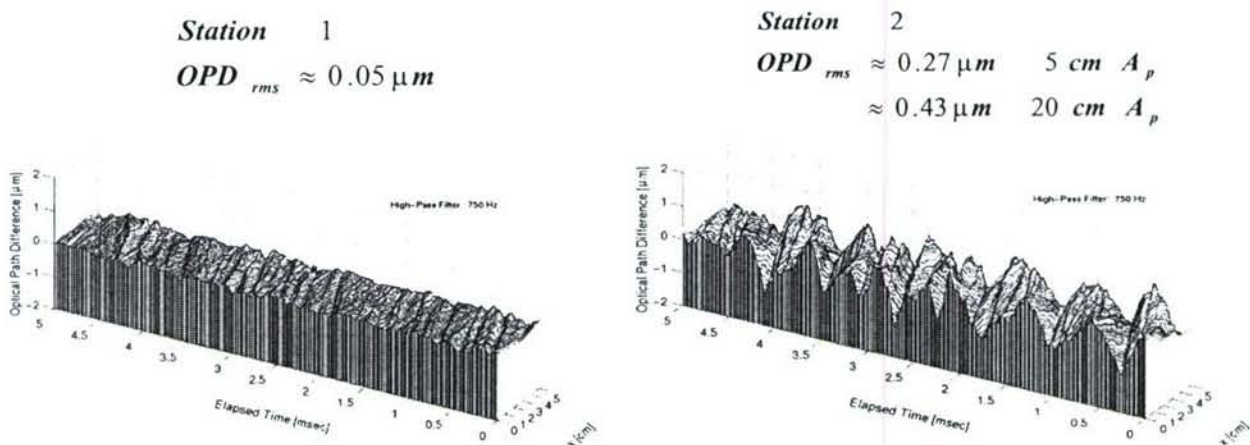


Figure 1. Wavefront Measurements Taken for Propagation through the AEDC Compressible Shear Layer Facility at a Simulated Flight Mach Number of 0.8 at 13,500 ft [Refs. 11,12].

Cause of Aero-Optic Aberrations. Not only were the AEDC data the first of their kind, the wavefronts at 0.5 m from the separation point presented a far-larger aberration environment than was expected due to the then-believed cause of the aberrations in turbulent shear layers. Discovering the cause of the aberrations became the objective of our second AFOSR grant and the result of that investigation led to the now universally-accepted cause referred to as the *Weakly-Compressible Model*.² The key realization at the heart of the Weakly-Compressible Model is the fact that because of the Kelvin Helmholtz instability, free shear layers naturally form coherent structures and, in a frame convecting with the layer, the flow in the coherent structures has high curvature (see Fig. 2).^{1,2} This curvature has a concomitant pressure gradient that lowers the pressure at the center of the structures (by several *psi* in the case of near-transonic shear layers). The low pressure is accompanied by a reduction in the density, which in turn lowers the index of refraction. It is this variation in the index of refraction due to the coherent flow structures and the accompanying high pressure/density in the braid connecting adjacent structures cause most of the aero-optic aberrations in weakly-compressible shear layers. As discussed in Reference 2, all other aberrating influences present in a shear layer, fed by a common total temperature, have effects that add up to only a small fraction of this principal cause. Although, this cause-and-effect explanation appears to be straightforward, it had long been thought (i.e., common knowledge) that static-pressure variations in a free shear layer were negligible, the so-called Strong Reynolds Analogy; the Weakly-Compressible Model argues exactly the opposite.

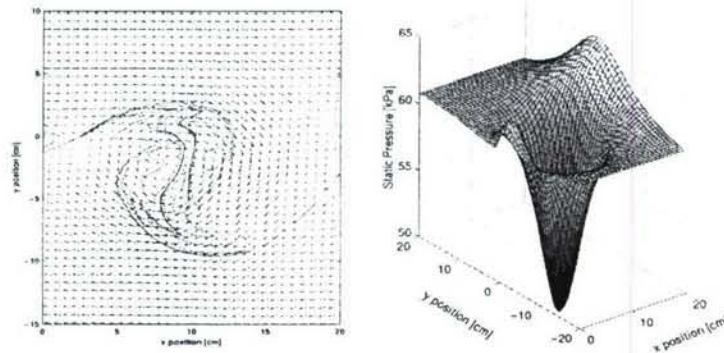


Figure 2. Coherent structure at an Instant in Time, its Flow field as seen in the Convective Frame and its Concomitant Pressure Well as Computed by the Weakly-Compressible Model [Ref. 2].

When the model was used to compute the AEDC conditions, it showed excellent agreement in the large-scale structures, but did not predict the higher-frequency aberrations on the wavefront data. Further analysis convinced us that the higher-frequency aberrations were due to the turbulent boundary layer over the extraction window of the tunnel. To simulate the addition of the boundary layer aberrations, an aberration time series from AEDC Station 1 (as that on the left of Fig. 1, which is due to a turbulent boundary layer) was added to the Weakly-Compressible Model predictions. The comparisons are shown in Fig. 3, which shows the simulation for the AEDC Station 2 conditions in the upper left hand, the AEDC Station 2 data in the lower right hand, and the result of adding the Station 1 wavefronts (upper right hand) to the simulations, resulting in the lower left hand time series.

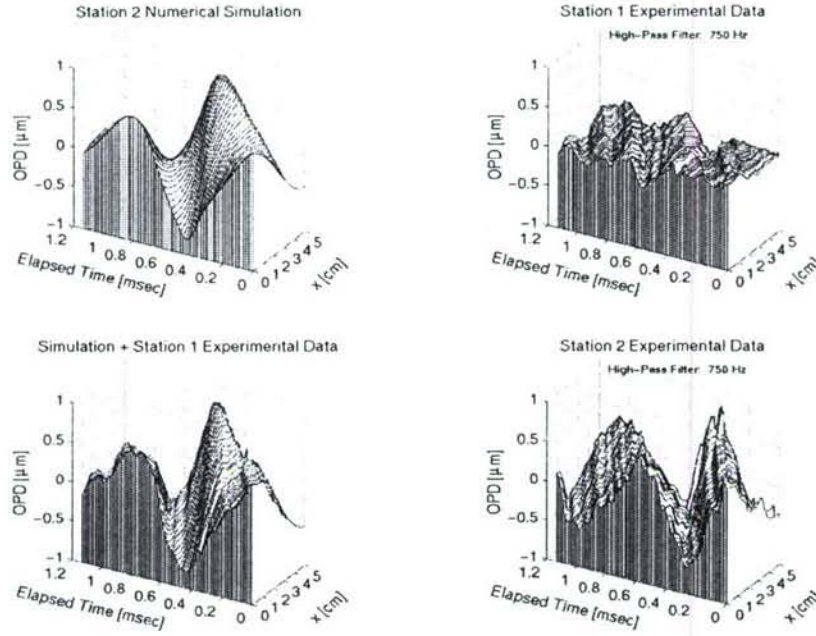


Figure 3. Example Time Series of Wavefronts: the Weakly-Compressible-Model-computed wavefronts for the AEDC, Station 2 conditions (upper left); compared to the Station 2 experimental wavefronts (lower right); when the Station 1 wavefronts (upper right) are added to the computed wavefronts, the comparison is even better (lower left) [Ref. 2].

It is clear that the two bottom time series, the simulation and the data, compare well.² Having the model enabled us to infer that the tilt in the Station 2 data was really a ramification of a larger coherent structure convecting past the 5 cm aperture used in the AEDC experiments. Using our model, we were also able to show that over the larger aperture the OPD_{rms} increases to $\sim 0.43 \mu\text{m}$, none of which can be removed by tilt corrections. In this case the Strehl ratio dropped to 0.011.¹³ Finally, with the help of the model, we were able to scale the aberration effects measured at the AEDC conditions over the small 5 cm aperture, not only to larger apertures, but also to other altitudes and Mach numbers.¹⁴

Based on the good agreement with the predicted aero-optic characteristics for the AEDC shear-layer and the measured wavefronts, it was clear that the most controversial assumption within the weakly compressible model was the setting aside of the Strong Reynolds Analogy. As such, in the last AFOSR grant a compressible shear layer facility was designed and constructed at Notre Dame to reproduce the shear layer at AEDC and used to validate the presence of pressure wells within the coherent structures in the shear layer. Figure 4 shows a flow visualization and measured pressure well within a coherent structure in a shear layer matching the AEDC conditions. Figure 4 may be compared to the weakly compressible model predictions in Figure 2.¹⁵

A final comment regarding aero-optic environments posed by flow around an airborne beam director, it is clear that the most degrading flow environment is due to separated flows. Referring to the Station 1 data in Figure 1, a turbulent boundary layer does induce aberrations on a laser passing through it; however, these aberrations are relatively small compared to that induced by propagation through a free shear layer.

Although the OPD_{rms} for propagation through a turbulent boundary layer is relatively low, it should be kept in mind that from time to time the instantaneous Strehl ratio (Eq. 1) can drop to near zero. Thus while the average Strehl ratio is high, some applications, such as free-space communication, may need to be concerned with turbulent boundary layers.

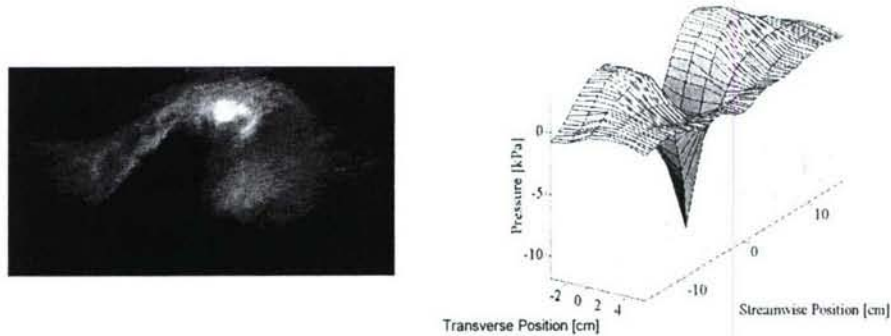


Figure 4. Experimental validation of the Weakly Compressible Model [Ref. 15].

Flow-Control, Feed-Forward Adaptive-Optic Foundations. Having now a physical explanation for the aberrating effects due to propagation through a free shear layer, it is possible to contemplate flow control approaches to mitigating its aero-optical effects. In fact, several Air Force Programs are presently investigating flow control influences on aero-optic environments. Many of these are specifically directed toward attempting to suppress the formation of large coherent structures in a shear layer by the introduction of smaller-scale disturbances into the shear layer near its separation point. On the other hand, Notre Dame has long advocated the use of flow control to regularize the shear layer in such a way that its aberrating structures become “regular” and predictable so that feed-forward approaches to adaptive optic corrections become tenable. It is well known that free shear layers are receptive to forcing at the separation point; Reference 4 is a review article on the topic. Based on the information contained therein, the most efficient approach to forcing a shear layer is at its most unstable frequency and this is the approach taken for the heated jet demonstration reported below. More recent results have shown that forcing can stabilize a shear layer over some distance (window);¹⁶ recall from the *Introduction* that Notre Dame inferred that stabilization meant regularization. In addition, the more recent literature contains other characteristics about the choice of forcing frequency. Figure 5 demonstrates that a shear layer can be caused to stay at the same thickness, that is to say, stabilize its thickness; further, these experiments were performed for relatively high Reynolds number shear layers, albeit for low Mach numbers.

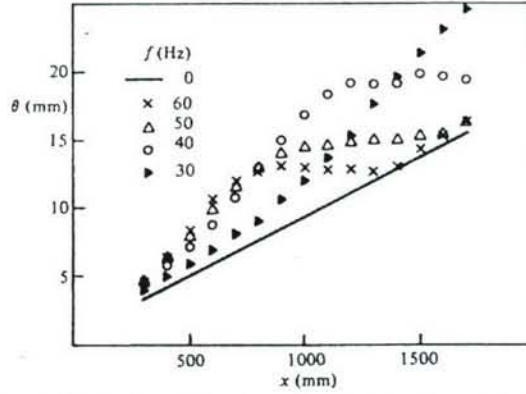


Figure 5. Evidence of the receptivity of a shear layer to forcing by oscillating a trailing edge flap [Ref. 16].

As shown in Figure 5, the choice of forcing frequency controls the location where the shear layer's thickness is stabilized. The lower forcing frequencies cause the shear layer to be controlled over a longer distance. This fact will be returned to when discussing our forcing experiments for the compressible shear layer. While the literature did not suggest that the shear layer became "regularized" in the sense that every structure convecting through this region is identical and its passage is periodic, the fact that the coherent structure size is related to the shear layer thickness implied to us that regularization was possible. If, indeed, shear layers could become regular and if the aberration patterns had a concomitant regularization, then making flow control part of the adaptive-optic scheme could allow a feed-forward adaptive optic correction that would defeat the bandwidth limitations imposed by wavefront sensing, conjugate computation and application, and any latencies present in the electronics associated with the deformable mirror and its drivers.

III. RESULTS

The major accomplishments of this grant were the successful demonstrations of feed-forward adaptive-optic correction of laser beams dynamically aberrated by propagation through aero-optic flows. These were accomplished by first demonstrating correction of a laser projected through a heated jet acoustically regularized in its near-nozzle-exit region. Simultaneous to the work on the heated jet, various flow control devices were used to try to regularize a compressible shear layer, eventually successfully stabilizing and regularizing the layer. Once controlled, the approach used for the heated-jet demonstration was used to correct for a laser propagated through the regularized compressible shear layer. These results will be described in three parts starting with the heated jet demonstration.

Heated-Jet Demonstration.

Regularized Shear Layer. The Notre Dame heated-jet facility has been in existence since our first aero-optic AFOSR grant. During that grant, it was found that the shear layers forming the two edges of the jet could be robustly regularized in the near-nozzle-exit region by using a speaker placed 1.0 m from the jet exit, as shown schematically in Figure 6 and described in detail in Reference 17.

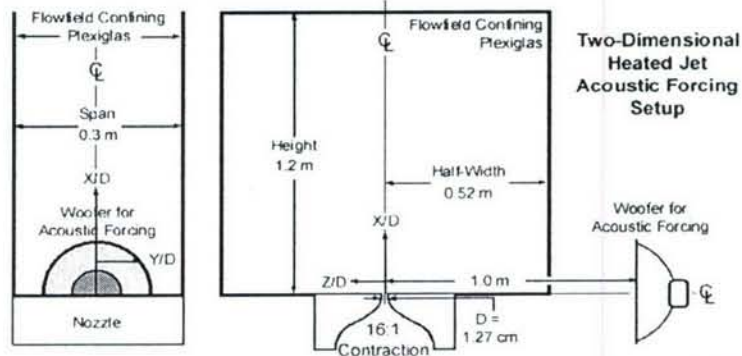


Figure 6. Schematic of the forcing scheme used on the Notre Dame heated jet [Ref. 17].

The frequency used to force the shear layer was chosen by measuring the natural, unforced center frequency of the layer using a Malley Probe.³ This frequency was shown to be the shear layers' most unstable frequency as computed using information in Reference 4, 240 Hz for the 7 m/s jet. This frequency was then used to drive a speaker with a sinusoidal signal. Figure 7 shows the result of the forcing in the form of a phase-locked temperature survey of the jet and a time series of wavefronts obtained by projecting an otherwise collimated laser through the jet over a 25 mm aperture centered at 25 mm from the nozzle exit plane. The wavefronts on the right of Figure 7 show that although the shear layer is being forced at 240 Hz, the wavefront repeat pattern is at 120 Hz, the forcing frequency's subharmonic. In a related numerical study,¹⁸ this 120 Hz repeat cycle was found to be due to vortex pairing downstream of the regularized region.

Adaptive-Optic Demonstration. An 18 mm diameter laser beam was projected perpendicular to and through our 240-Hz acoustically-forced heated jet described above.

Wavefront sensors were used to determine the character of the laser beam's aberrated wavefront. Although not precisely 1-D, phase-lock-averaged wavefronts were sufficiently 1-D so that a cross-stream averaged representation of the wavefront closely matched the wavefront over the full aperture. The phase-locked, cross-stream-averaged 1-D wavefronts' spatial and temporal characters were then fit with a two-harmonic analytic model using optimization routines.

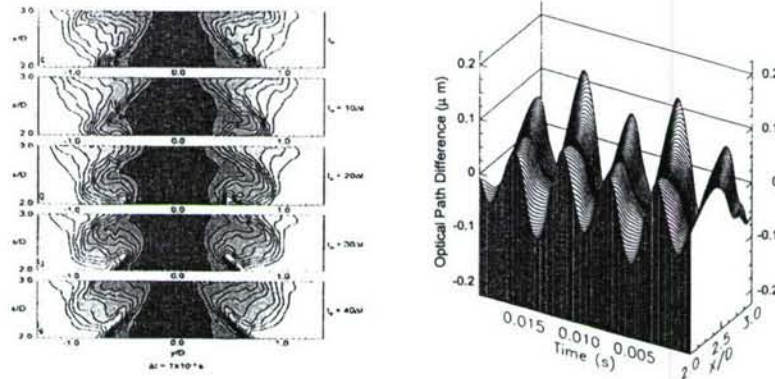


Figure 7. Selected succession of phase-locked-averaged temperature fields for the acoustically-forced heated jet (left) and a time series of wavefronts for propagation through and same jet (right) [Ref. 19].

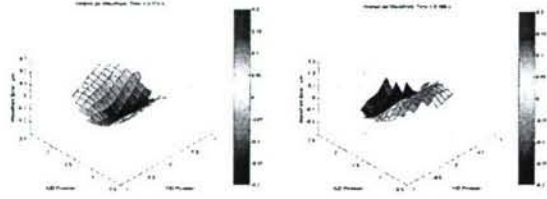
Although two harmonics (i.e., Fourier modes) did not fully characterize the forced waveform, a simulation performed during the experimental design demonstrated that the two-harmonic conjugate waveforms would do a reasonably-good job in correcting the imprinted aberrations from the forced heated jet. The conjugate waveforms derived from the two-harmonic analytic function were loaded into a waveform generator and sent to the amplifiers that drive the deformable mirror. After reflecting off the mirror, we found that most of the diffraction-limited integrity of the beam could be restored and maintained for extended periods of time. Figure 8 shows four wavefronts collected during the demonstration at two phase angles, the top two wavefronts for the uncorrected beam and the bottom two wavefronts after correction.²⁰ Also shown in Figure 8 are the concomitant far-field intensity patterns for a laser wavelength of $0.63 \mu m$. These two frames represent the most stressing phase angles for correction.

Far-field patterns like those in Figure 8 were then used to compute the Strehl ratio using the strict definition of Strehl ratio, i.e., Eq. (1), and by taking the highest intensity in the far field regardless of location (pseudo-Strehl ratio). The results are shown in Figure 9. On a time averaged basis, the Strehl ratio was restored from ~ 0.65 to ~ 0.9 . It should be kept in mind that the OPD_{rms} for the uncorrected aberrations due to propagation through the heated jet is only $0.11 \mu m$. This demonstration, in fact, set a milestone in adaptive optics. Our now-demonstrated adaptive-optic correction using our flow-control approach, even this relatively-low bandwidth experiment with a clearing frequency of only 240 Hz, would have required a 2.4 kHz loop-closing system, approximately an order of magnitude faster than state-of-the-art, traditional adaptive-optic systems.

There are a number of observations that were drawn from this experiment that affected our approach to a similar demonstration for the compressible-shear-layer. In the heated-jet experiment, the conjugate waveform was sent to the mirror by feeding forward

the analytic two-harmonic model we had predetermined should do a reasonably-good job of correcting the beam's aberrations. The model allowed for adjusting the amplitudes and phases of the two-harmonic wavefronts to match the experimentally-obtained, phase-averaged wavefronts from the forced heated jet. Also the model had an additional component, its phase delay from a trigger signal from the flow-control forcing signal (speaker).

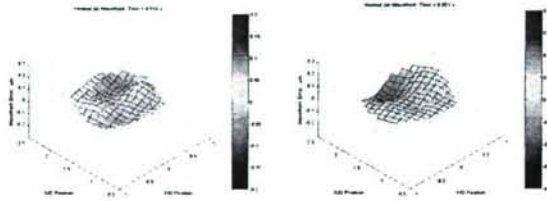
Uncorrected Wavefronts



Phase = 90°

Phase = 180°

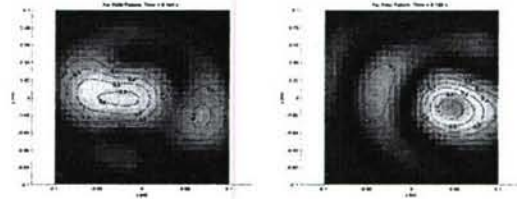
Adaptive-Optically Corrected Wavefront Images



Phase = 90°

Phase = 180°

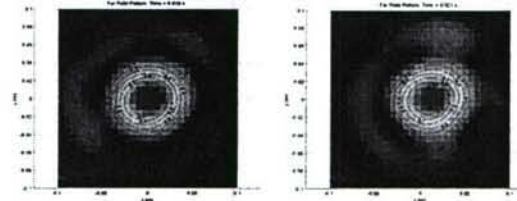
Uncorrected Far-Field Images



Phase = 90°

Phase = 180°

Adaptive-Optically Corrected Far-Field Images



Phase = 90°

Phase = 180°

Figure 8. Instantaneous wavefronts and concomitant far-field patterns ($\lambda = 0.63 \mu\text{m}$) at two selected phase angles [Ref. 17].

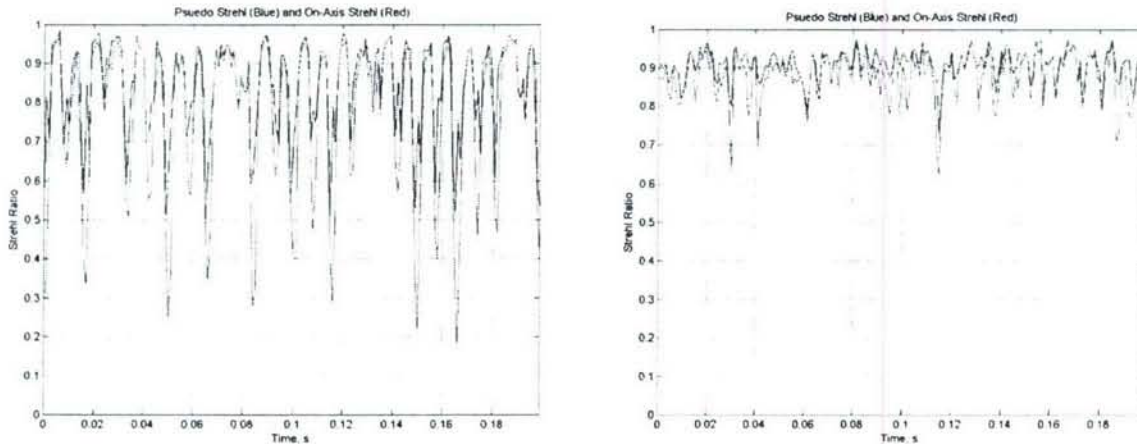


Figure 9. Time history of Strehl ratio (the curves with the lowest values) and pseudo-Strehl ratio without (left) and with (right) adaptive-optic correction ($\lambda = 0.63 \mu\text{m}$) [Ref. 17].

In the heated-jet experiment the final slow feedback loop was provided by a man in the loop. By the time we performed the experiment, this man-in-the-loop part of the experiment was our biggest unknown; however, the learning process in this part of the experiment was instructive in forming the basis for possible automated approaches to the outer loop and in guiding us in the compressible-shear-layer demonstration. The proper

phase delay had to be synced up with the forced heated jet. To perform this function, the residual wavefront error's centroid locations from the Hartmann sensor were observed by the operator at the monitor scan rate of 30 Hz. With the model out of proper phase, these centroids were seen to jump around. As mentioned above, the aberration pattern repeat was 120 Hz even though the shear-layer was forced at 240 Hz. In order to sync the correction, the deformable-mirror driving frequency was adjusted to 240.1 Hz while continuing to drive the shear layer at the 240 Hz; this caused the observed Hartmann sensor centroids to go through a 10-second cycle of maximizing and minimizing their position patterns. Once the operator perceived that the pattern was minimized the deformable-mirror driving signal was reset to 240 Hz with the correct phase delay. The effect of going in and out of synchronization at the beat frequency can be seen in Figure 10, which shows the Strehl ratio with the beat frequency set at 1 Hz.

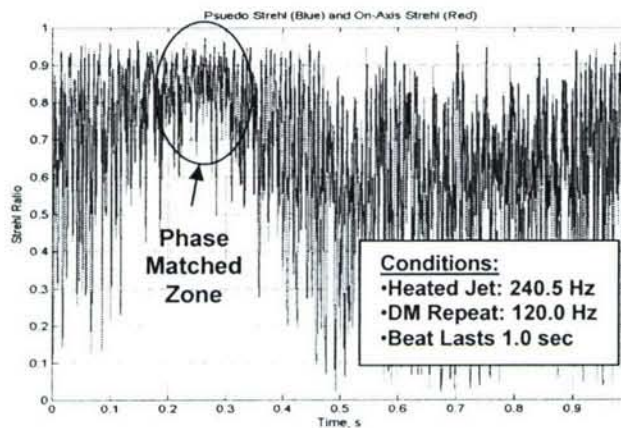


Figure 10. Demonstration of the Beat-Frequency Approach to Feedback Optimization [Ref. 17].

From a scaling point of view, the heated-jet demonstration was approximately a one-fourth-bandwidth simulation of the required bandwidth for correction of a laser propagated through the compressible shear layer. The coherence length for a typical structure to be corrected in the compressible shear layer was roughly 10 times that for the heated jet and the shear layers velocity roughly 40 times that of the heated jet so that required was expected to be roughly 4 times that for the heated jet. In the heated jet, the maximum peak-to-peak aberration was $< 0.2 \mu\text{m}$ while the compressible shear layer's maximum peak-to-peak aberrations was expected to be $\sim 1.5 \mu\text{m}$ (see Figure 1). This scale up of roughly 5 in OPD amplitude had a number of implications toward wavefront sensing and adaptive-optic correction. In fact, the sensitivity of the wavefront sensor and the precision in the mirror correction are less stressing for the compressible shear layer experiment; in the case of the heated jet, both were at the lower end of their capabilities. Our Xinetics deformable mirror was specifically designed to be able to have a $4 \mu\text{m}$ dynamic range, which translates to the ability to correct up to an $8 \mu\text{m}$ aberration (i.e., a $4 \mu\text{m}$ displacement on the mirror imposes an $8 \mu\text{m}$ aberration on a planar wavefront reflected off the mirror). The scale up in frequency to around 1 kHz was well within the bandwidth of the mirror, which had been designed to be linear out to $\sim 5 \text{ kHz}$; however, the driver amplifiers had a latency that had to be included in the phase delay. Thus, our success in correcting for laser propagation through the heated jet translated into a high

confidence that the same could be done for the compressible shear layer if the shear layer could be regularized.

Shear Layer Forcing. After trying to force the shear layer with only marginal success using a variety of actuators including plasma actuators²⁰, we were beginning to wonder whether robustly stabilizing compressible shear layers was possible since we found no other reference to having done it for high Mach numbers. Eventually we were able to find a combination of facility, actuator and forcing frequency that led to robust control of the shear layer. In terms of the facility, we ended up redesigning and building a new compressible shear layer tunnel. Figure 11 shows a picture of the redesigned shear layer facility. The new design included a new inlet for a wider test section and included a downstream throat to choke the flow and prevent pressure disturbances from the vacuum pumps from propagating into the test section.²¹

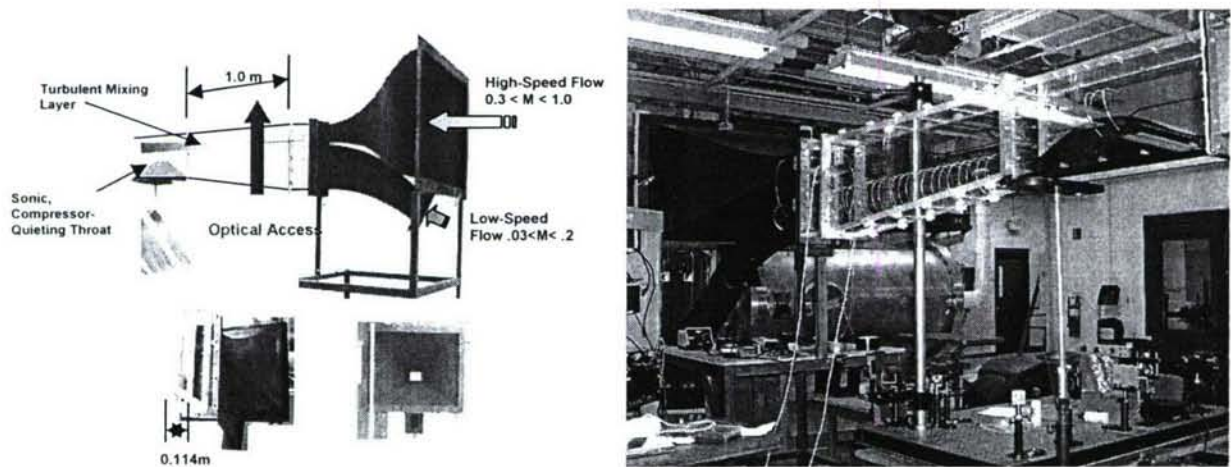


Figure 11. New Compressible Shear Layer Facility [Ref. 21].

The key to successful shear layer control was due to two factors, the first of which was finding an actuator. The most robust actuators found were voice-coil actuators made from 1 Watt speakers with one side cut so that the diaphragm was free to move perpendicular to the flow direction. The amplitude of the motion was as high as 1 mm for the lower frequencies (< 500 Hz) rapidly dropping off with increasing frequency. The actuators mounted in the shear layer splitter plate are shown in Figure 12.

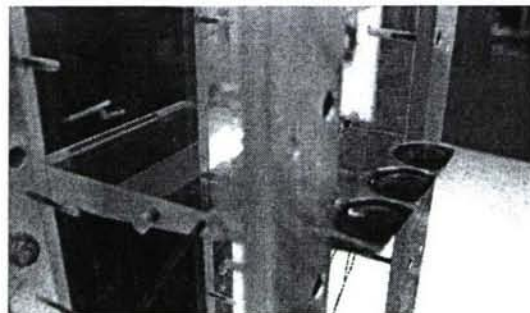


Figure 12. Voice-coil actuators mounted at the edge of the shear-layer splitter plate.

The second factor in our success was a realization that once recognized was present in the literature, but was not obvious to us until we had a chance to examine the results from numerical simulations of a forced shear layer. Figure 13 shows some of the numerical results for a compressible shear layer at conditions similar to the AEDC flow conditions but with a feeding boundary layer that is approximately twice that of the AEDC flow. On the left is the “natural” center frequency of the unforced shear layer computed from the numerical results using

$$f_n(x) = \frac{\int PSD(f, x) f df}{\int PSD(f, x) df} \quad (2)$$

These frequencies match the expected characteristics of an experimental shear layer with the highest frequency closest to the splitter plate, with the most unstable frequency in this case being ~ 1.4 kHz. On the right is the momentum thickness versus distance from the splitter plate similar to the results in Figure 5, but for the near-AEDC conditions. The solid line is the shear layer growth for the unforced shear layer. The significance of these two figures taken together is that they are instructive in attempting to regularize shear layers. The first message is that forcing the shear layer at a frequency that would occur in the unforced shear layer at some location downstream causes the shear layer to regularize for some distance upstream of that location; once the location is reached where that frequency occurs naturally, the shear layer begins to grow again, i.e., loses regularization. So the location and extent of where the shear layer is to be regularized depends on the distribution of natural frequencies present in the unforced case. The second message is that the shear layer is receptive to forcing at *significantly-lower frequencies* than its most unstable frequency.

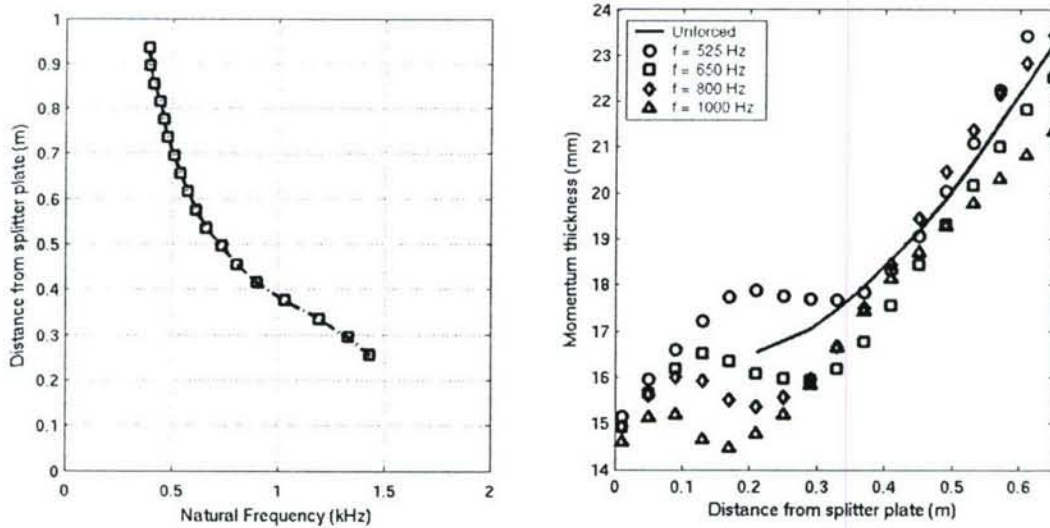


Figure 13. Numerical results showing shear layer characteristics for a shear layer at flow conditions similar to the AEDC conditions.

These observations were critical to our success in forcing our experimental shear layer. Prior to studying the numerical results, we had been trying to force the shear layer at higher frequencies, nearer the shear layer’s most unstable frequency, based on our experience with the heated jet. All of the mechanical actuators we had investigated

became less efficient at the higher frequencies with the possible amplitudes falling off at roughly the square of the driving frequency. Further, we had misread the data available in the literature thinking that the forcing strategy was to force at the naturally-occurring frequency at the location and beyond that we were trying to control. Once we began forcing the shear layer at the lower frequencies, we began to see better and better regularization. The simulations also justified our inference that stabilization equates to regularization. Another result that we observed in the numerical simulations was the cause for the subharmonic repeat cycle that we had observed in the heated-jet experiments. Figure 14 shows the rollup pattern for the shear layer every cycle on the left and every other cycle on the right at the same phase angle.²² Notice that it is the pairing event that causes a stretching effect in the shear layer every other cycle.

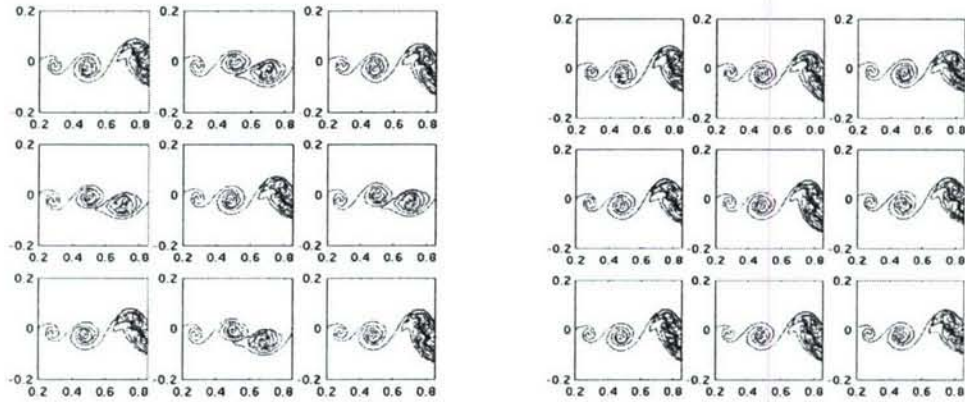


Figure 14. Numerically-predicted rollup patterns in a forced shear layer, every cycle at same phase angle (left) and every other cycle (right) [Ref. 22].

Based on our new insight into forcing compressible shear layers we were eventually successful in robustly regularizing our shear layer running with the high-speed side at \sim Mach 0.8 and the low-speed side running at \sim Mach 0.1. The regularization is documented by recording hundreds of wavefronts triggered every 30° of phase, phase locked to the forcing signal. Phase-locked-averaged wavefronts from this series are shown in Figure 15.²¹ A single phase angle is shown in detail on the right side of the Figure.

Regularization was shown to be possible using a variety of actuators, the most effective being the voice-coil actuators described earlier; however, piezoelectric bimorph actuators were also shown to work relatively well. The problem with the bimorph actuators was that in order to achieve amplitudes comparable to the voice-coil actuators, the bimorph actuators had to be “tuned” so that their natural frequencies matched the desired forcing frequency. This required the actuators to be rigidly bonded to the trailing edge of the splitter plate with the length of the actuator extending past the trailing edge by a length that had to be experimentally determined.

It should also be noted in the wavefronts in Figure 15 are for an aperture size that captures only about half a cycle; the streamwise length of the half cycle being \sim 10 cm (\sim 4 in). The wavefronts in Figure 15 have tilt removed so that they appear to present a “breathing” of the wavefront. When tilt is included, it is clear that a near-sinusoidal waveform is seen to convect through the 4 inch aperture.

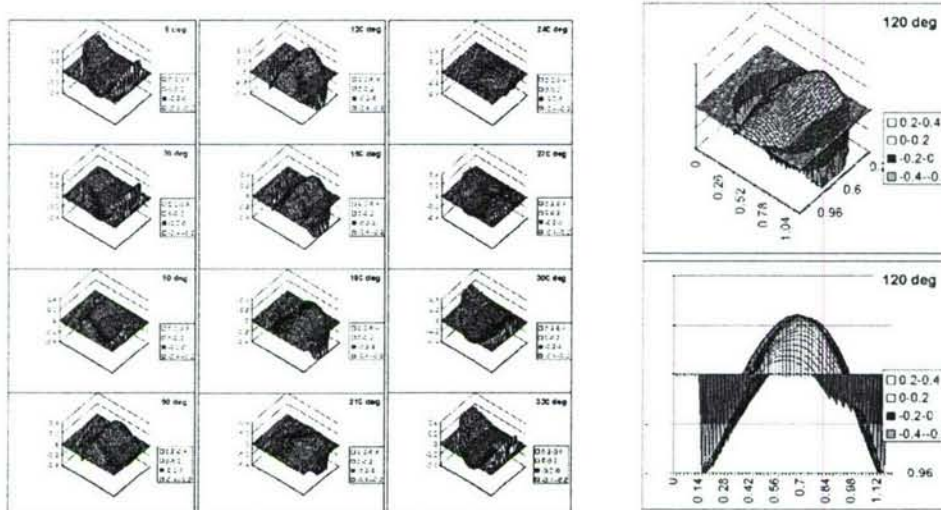


Figure 15. Voice-coil actuator, phase-lock-averaged wavefronts every 30°, and a single wavefront at 120° [Ref. 21].

Adaptive-Optic Correction. Once the wavefronts were obtained, conjugates were constructed and overlaid, as a function of phase angle, onto our deformable-mirror's actuator locations. Then time (phase-angle) series of actuator displacements were constructed for each actuator. These displacement phase-angle series were then converted to voltage waveforms and loaded into memory in a waveform generator for each of the 37 mirror actuators. The mirror was then run and its conjugate waveform measured and compared to the conjugate of the measured wavefronts from the regularized shear layer. By the morning of 10 July 2006, we knew it was simply a matter of combining all of the various components to perform a correction demonstration. The demonstration was run that afternoon. One example data series from that demonstration is shown in Figure 16. Figure 16 shows a series of OPD_{rms} wavefront error over an entire cycle of phase angles with the Mirror running a range of delays from the forcing signal trigger. As can be seen in the figure, when the mirror is properly phase delayed, the error drops to just over 0.1 μm (240°-270°).

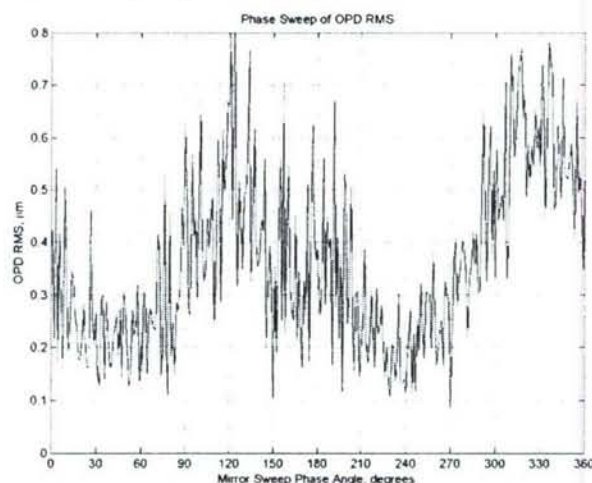


Figure 16. Residual Wavefront Error as a function of deformable-mirror phase delay (10 July 2006).

The data in Figure 16 is for the case of using a 4 inch aperture and correcting for only half of a full cycle of disturbance. The experiment was repeated using an 8-inch Schmidt-Cassegrain where the a full cycle of aberration in the streamwise direction was removed. Since the tunnel is only 4.5 inches wide, the wavefronts were clipped to a rectangular aperture 7.5 in X 4 in. The Strehl ratios for this new Schmidt-Cassegrain experiment results are shown in Figure 17. Figure 17 data is based on individual wavefronts taken with a phase-locked pulsed laser with a 3 ns pulse length. The Strehl ratio was constructed from far-field reconstructions for a 1 μm laser and the on-axis intensity after tilt removal was divided by the diffraction-limited, on-axis intensity for a 7.5 in X 4 in aperture; two selected far-field patterns, one uncorrected and one corrected, are shown in Figure 18. The residual OPD_{rms} error in the corrected second series was the same as that for the 10 July experiment, $\sim 0.1 \mu\text{m}$. Close analysis of the wavefronts and boundary-layer measurements showed that of the OPD_{rms} residual error of $\sim 0.1 \mu\text{m}$, approximately 0.07 of it was due to the turbulent boundary layer on the high-speed wall of the tunnel at the beam-extraction window.

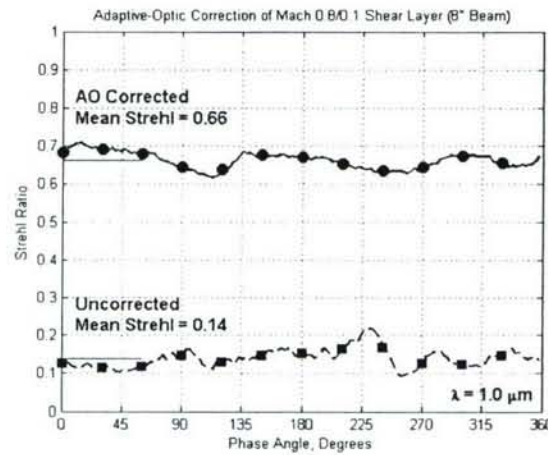


Figure 17. Strehl Ratio for an 8 inch diameter laser beam projected through a Mach 0.8 separated shear layer with and without Notre Dame's Feed-Forward AO approach

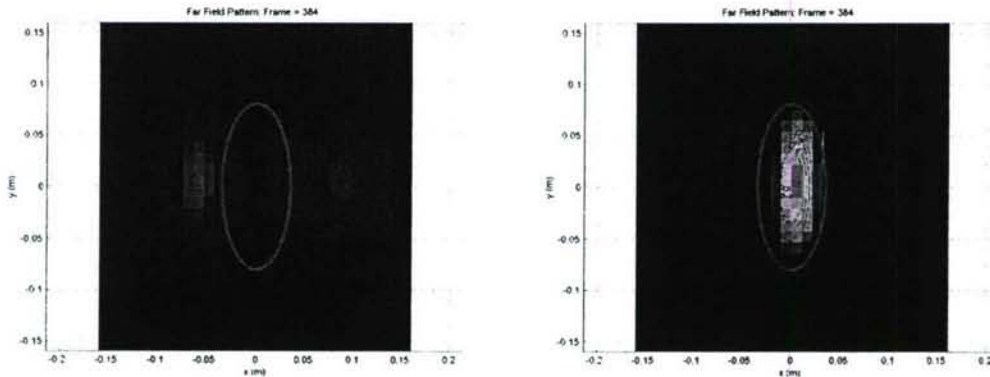


Figure 18. Example Far-Field irradiance patterns for uncorrected laser propagation through our Mach 0.8 separated shear layer (left) and for AO-corrected propagation (right) for a $\lambda = 1.0 \mu\text{m}$ laser.

IV. CONCLUSIONS

This effort is able to claim at least 3 major historic milestones: performing the first ever adaptive-optic correction of a laser propagated through an aero-optic flow field and in so doing perform the highest-bandwidth adaptive-optic correction; the second is the verification that shear-layer thickness stabilization is presumptive evidence of regularization and the first-ever regularization of a high-Mach-number shear layer; the third is the first-ever adaptive-optic correction of a laser propagated through a Mach 0.8, flight-relevant separated shear layer. These historic milestones are the result of a progression of breakthroughs made during a series of AFOSR-supported research in aero-optics performed at Notre Dame. These milestones have been tabularized in Figure 19, showing the history of discovery in aero-optics, a field of study that had been declared in the late 1980's as being a mature discipline with nothing left to be learned.

Chronicle of Notre Dame's Progress on AFOSR-Sponsored Research Directed toward AO Mitigation of Aero-Optic Disturbances

1995	Notre Dame develops the first truly high-bandwidth wavefront sensor with 100+kHz capture rates, the SABT Wavefront Sensor
1995	In cooperation with personnel at Arnold Engineering and Development Center (AEDC) Notre Dame captures long time series of high-bandwidth correlated wavefronts for propagation of a 5 cm laser beam through a Mach 0.8 separated Shear Layer
1997	Notre Dame proposes a physical cause of shear-layer induced Aero-Optic disturbances, the Weakly-Compressible Model
1999	Notre Dame experimentally validates the most controversial element of the Weakly-Compressible Model, large pressure wells formed in the coherent vortical structures that form naturally in a shear layer due to the Kelvin-Helmholtz instability.
1999	Notre Dame demonstrates the use of POD Eigen modes to predict the wavefront-aberrating character of a forced, heated-jet shear layer.
2000	Notre Dame begins studying a feed-forward approach to Adaptive-Optic corrections of an aero-optic disturbance.
2000	Notre Dame begins design and procurement of a specially-tailored Adaptive-Optic system capable of meeting the requirements of a feed-forward correction of the aero-optic environment imposed by a transonic shear layer.
2002	Notre Dame achieves marginal success in forcing compressible shear layers up to Mach 1.1.
2005	In a historic demonstration, Notre Dame demonstrates real-time adaptive-optic correction of a 240 Hz forced aberration in its heated jet, peaking the Strehl ratio from 0.4 to 0.9 for a HeNe laser.
2006	Notre Dame achieves robust flow control of a Mach 0.8 shear layer using voice-coil actuators in its newly-designed compressible shear-layer facility.
2006	on July 10 th , Notre Dame successfully demonstrates the world's first correction of a laser beam projected through a flight-relevant Mach and Reynolds number free shear layer.

Figure 19. Progress in AFOSR-sponsored, aero-optic research at Notre Dame.

REFERENCES

1. Jumper, E.J., and Fitzgerald, E.J., "Recent Advances in Aero-Optics," *Progress in Aerospace Science*, **37**, 2001, pp. 299-339.
2. Fitzgerald, E.J. and Jumper, E.J., "The Optical Distortion Mechanism in a Nearly Incompressible Free Shear Layer," *Journal of Fluid Mechanics*, **512**, 204, pp. 153-189
3. Gordeyev, S., Jumper, E.J., Ng, T. and Cain, A., "Aero-Optical Characteristics of Compressible, Sub-Sonic Turbulent Boundary Layers," AIAA Paper 2003-3606.
4. Ho, C-M, and Huerre, P., "Perturbed Free Shear Layers," *Annual Reviews of Fluid Mechanics*, **16**, 1984, pp. 365-424.
5. Smith, W.J., *Modern Optical Engineering: the Design of Optical Systems*, McGraw-Hill, New York, 1966.
6. Gilbert, K. and Otten, J. (eds), *Aero-Optical Phenomena*, Progress in Astronautics and Aeronautics Series, **80**, AIAA, Inc., New York, 1982.
7. Tatarski, V.I., *Wave Propagation in Turbulent Medium*, Dover, New York, 1961.
8. Tyson, R.K., *Principles of Adaptive Optics*, Academic Press, Inc., San Diego, 1991.
9. Tyson, R.K., "The status of astronomical adaptive optics systems," O.E. Reports, 121, pp. 11,13, Jan 1994.
10. Hugo, R.J., and Jumper, E.J., "Experimental measurement of a time-varying optical path difference by the small-aperture beam technique," *Applied Optics*, **35**, pp. 4436-4447, August 1996.
11. Jumper, E.J., Hugo, R.J., Havener, G. and Stepanek, S.A., "Time-Resolved Wavefront Measurements through a Compressible Free Shear Layer," *AIAA Journal*, **35**(4), April 1997, pp. 4436-4447.
12. E. J. Fitzgerald and E. J. Jumper, "Aperture Effects on the Aero-Optical Distortions Produced by a Compressible Shear Layer," *AIAA Journal*, **40** (2) February 2002, pp. 267-275.
13. Cicchiello, J.M., Fitzgerald, E.J. and Jumper, E.J., "Far-Field Implications of Laser Transmission Through a Compressible Shear Layer," *Free-Space Laser Communication Technologies XIII Conference*, **4272**, SPIE, San Jose California, 20-26 January 2001, pp. 245-259.
14. Fitzgerald, E.J. and Jumper, E.J., "Scaling Aerooptic Aberrations Produced by High-Subsonic-Mach Shear Layers," *AIAA Journal*, **40** (7), July 2002, pp. 1373-1381.
15. Chouinard, M. Asghar, A., Kirk, J.F., Siegenthaler, J.P. and Jumper, E.J., "An Experimental Verification of the Weakly-Compressible Model," AIAA Paper 2002-0352, Jan 2002.
16. Oster, D. and Wygnanski, I., "Forcing Mixing Layers Between Parallel Streams," *Journal of Fluid Mechanics*, **123**, 1982, pp. 91-130.
17. Duffin, D.A., "Feed-Forward Adaptive-Optic Correction of Aero-Optical Aberrations Caused by a Two-Dimensional Heated Jet," AIAA Paper 2005-4776, June 2005.

18. Nightingale, A. Gordeyev, S., Siegenthaler, J., Wittich, D, and Jumper, E., "Computed Aero-Optic Characteristics of a Free Shear layer using the Weakly-Compressible Model," *Proceedings of the Directed Energy Professional Society*, Monterey California, March 2006.
19. Hugo, R.J. and Jumper, E.J., "Applicability of the Aero-Optic Linking Equation to a Highly Coherent, Transitional Shear Layer," *Applied Optics*, **39** (24), August 2000, pp. 4392-4401.
20. Siegenthaler, J.P., Jumper, E.J., and Asghar, A., "Preliminary Study in Regularizing the coherent Structures in a Planar, Weakly-Compressible, Free Shear Layer," AIAA Paper 2003-0680, Jan 2003.
21. Rennie, R.M., Siegenthaler, J.P. and Jumper, E.J., "Forcing of a Two-Dimensional, Weakly-Compressible Subsonic Free Shear layer," AIAA Paper 2006-0561, January 2006.
22. Nightingale, A., Gordeyev, S., Jumper, E.J., Goodwine, B. and Siegenthaler, J., "Regularizing Shear Layer for Adaptive Optics Control Applications," AIAA Paper 2005-4774, June 2005.